Applied Catalysis B: Environmental 125 (2012) 35–40

Contents lists available at SciVerse ScienceDirect

Applied Catalysis B: Environmental

journal homepage: www.elsevier.com/locate/apcatb

Visible light induced photosensitized degradation of Acid Orange 7 in the suspension of bentonite intercalated with perfluoroalkyl perfluoro phthalocyanine zinc complex

Dominik Drozd[a], Krzysztof Szczubiałka[a], Łukasz Łapok[a], Michał Skiba[b], Hemantbhai Patel[c], Sergiu M. Gorun[c], Maria Nowakowska[a,*]

[a] Faculty of Chemistry, Jagiellonian University, Ingardena 3, 30-060 Kraków, Poland
[b] Institute of Geological Sciences, Jagiellonian University, Oleandry 2a, 30-063 Kraków, Poland
[c] Seton Hall University, Department of Chemistry and Biochemistry, 400 South Orange Ave, South Orange, NJ 07079, USA

ARTICLE INFO

Article history:
Received 5 April 2012
Received in revised form 17 May 2012
Accepted 18 May 2012
Available online 27 May 2012

Keywords:
Bentonite
Perfluoroalkyl perfluoro-phthalocyanine
Azo dyes
Hybrid photosensitizer
Singlet oxygen

ABSTRACT

We report the intercalation of a perfluoroalkyl perfluoro phthalocyanine zinc complex ($F_{64}PcZn$) in bentonite (Ben) to generate a hybrid photosensitizer ($F_{64}PcZn \in Ben$) and demonstrate its ability to degrade a model azo dye, Acid Orange 7 (AO7), in aqueous solution using visible light. The $F_{64}PcZn$ photosensitizer is active both in the presence and in the absence of O_2, via the photogeneration of singlet oxygen or via a photoinduced electron transfer from the azo dye, respectively. Both $F_{64}PcZn$ and $F_{64}PcZn \in Ben$ exhibit high photochemical stability. The heterogeneous system can be used cyclically by the removal and reutilization of the photocatalytic hybrid, thus highlighting possible technological applications.

1. Introduction

Azo dyes are the most widely utilized synthetic colorants (60–70%), employed in textile, printing, leather, food, pharmaceutical, and agrochemical industries. Wastewaters generated from these industries, however, are heavily contaminated, for example those generated by the textile industries contain about 15% of the dyes used in the manufacturing process [1]. Contaminated wastewaters seriously threaten ecosystem since azo dyes are toxic, carcinogenic and resist biodegradation [1]. Their removal is subject to continuous research including via oxidations [2–6]. Promising photochemical oxidations using mostly the anatase polymorph of TiO_2, have been explored extensively and shown to be quite effective [7]. This process involves the photogeneration of valence holes and conduction-band electrons that react with chemisorbed oxygen generating reactive oxygen species, such as $O^{-}{}_2{}^{\bullet}$ ($HO_2{}^{\bullet}$) and $OH^{\bullet}$ radicals, which, in turn, react with dye molecules leading to their degradation [8,9]. In addition, the oxygen vacancies/positive holes, which are radical cations, also oxidize contaminants [10–18]. However, the anatase wide band-gap of about 3.2 eV limits its utility due to the lack of light absorption in the visible region. Doping TiO_2 with both metals and non-metals mitigates to a certain extent this problem.

An alternative approach consists of a dye–TiO_2 composite, in which an electron is transferred from an initially excited dye molecule to the conduction band of an aqueous suspension of TiO_2 resulting in the formation of $O^{-}{}_2{}^{\bullet}$ ($HO_2{}^{\bullet}$) and $OH^{\bullet}$ radicals as well as $^1O_2$. The activated oxygen species then oxidize contaminants present in water. The mechanism of this process, while different from the one described previously, is relatively inefficient [18].

Recently, cerium dioxide (CeO_2) has been shown to be a more efficient photosensitizer for dye degradation, including Acid Orange 7 (sodium 4-[(2E)-2-(2-oxonaphthalen-1-ylidene)hydrazinyl]benzene-sulfonate, AO7) [19]. The degradation mechanism, similar to that proposed above, namely dye self-sensitization, occurs via electron injection by photoexcited AO7 into cerium 4f orbitals. The reduction of surface oxygen leads

Abbreviations: Ben, bentonite; $F_{64}PcZn$, a perfluoroalkyl perfluoro phthalocyanine zinc complex; $F_{64}PcZn \in Ben$, a hybrid photosensitizer based on a perfluoroalkyl perfluoro phthalocyanine zinc complex intercalated in bentonite; AO7, Acid Orange 7; XRD, X-ray diffraction; RNO, N,N-dimethyl-4-nitrosoaniline; RH, relative humidity; DMF, dimethylformamide; MeCN, acetonitrile; ANS, 2-anthracene sulfonate.

* Corresponding author. Tel.: +48 12 6632250; fax: +48 12 6340515.
E-mail addresses: szczubia@chemia.uj.edu.pl (K. Szczubiałka), sergiu.gorun@shu.edu (S.M. Gorun), nowakows@chemia.uj.edu.pl (M. Nowakowska).

0926-3373/$ – see front matter © 2012 Elsevier B.V. All rights reserved.
http://dx.doi.org/10.1016/j.apcatb.2012.05.021

next to the formation of reactive oxygen species which oxidize a dye molecule. The role of CeO_2 is that of a mediator of electron-transfer from photo excited dye molecules to surface-bonded oxygen.

The generation of oxygen active species, aimed at the deep oxidation of dyes in solution can also be achieved via the photo-Fenton processes, in which hydrogen peroxide is catalytically decomposed using Fe^{3+} or ZnO and UV light [20].

Materials based on phthalocyanines intercalated into bentonite have been reported and used as catalysts for the polymerization of methyl methacrylate [21,22] and synthesis of styrene [23]. Reports on photocatalysts obtained from phthalocyanines and bentonite are quite scarce. Thus, aluminum phthalocyanine chloride was inserted into the interlamellar spaces of bentonite modified with cetyltrimethylammonium bromide [24]. The hybrid photocatalyst was found to degrade phenol and chlorinated phenols, but its efficiency decreased in time and upon recycling. A better stability has been reported for a trichlorophenol degradation photocatalyst prepared by intercalating hydrophilic palladium (II) phthalocyanine sulfonate in bentonite, but the metal complex was found to block the substrate adsorption [25].

We report here that a hydrophobic, C—H bonds-free, fluoro-fluoroalkyl phthalocyanine photosensitizer, zinc 1,4,8,11,15,18,22,25-octakis-fluoro-2,3,9,10,16,17,23,24-octakis-perfluoro(isopropyl)phthalocyanine (F_{64}PcZn) can be encapsulated into the naturally occurring clay phyllosilicate bentonite (Ben) and that the resulting hybrid material, F_{64}PcZn∈Ben, degrades an external substrate, the AO7 azo naphthol dye, without noticeable self-degradation.

2. Experimental

2.1. Materials

Bentonite (Sigma–Aldrich) containing >80% of pure smectite was used as received. Perfluoroalkylethyl thiohydroxypropyl-trimethylammonium chloride (Masurf® FS-1620) was purchased from Mason Chemical Company. F_{64}PcZn was synthesized as reported previously, by reacting perfluoro-4,5-di-(isopropyl)phthalonitrile obtained from perfluorophthalonitrile and perfluoropropene with zinc acetate [26,27]. Sodium anthracene-2-sulfonate (ANS) was prepared by reducing sodium anthraquinone-2-sulfonate (HPLC, Sigma–Aldrich) with Zn dust in the presence of NH_4OH. Potassium tetrathiocyanatodiamminechromate (III) ($K[Cr(NH_3)_2(SCN)_4]$) used in actinometric measurements, was obtained from ammonium tetrathiocyanatodiamminechromate (III) (Reinecke's salt, $NH_4[Cr(NH_3)_2(SCN)_4]$ H_2O, analytical grade, Sigma–Aldrich) and purified according to a literature procedure [28]. Iron (III) nitrate nonahydrate (analytical grade, Sigma–Aldrich) and perchloric acid (70%, Riedel-de Haën AG) were also used for actinometry. Imidazole (analytical grade, Sigma–Aldrich), N,N-dimethyl-4-nitrosoaniline (RNO, 97%, Sigma–Aldrich), potassium nitrate (analytical grade, POCh Gliwice). methanol (analytical grade, Lach-Ner), acetonitrile (analytical grade, Lach-Ner), dimethylformamide (analytical grade, Lach-Ner) were used as received.

2.2. Synthesis of F_{64}PcZn – bentonite photosensitizer (F_{64}PcZn∈Ben)

F_{64}PcZn∈Ben was synthesized by dispersing F_{64}PcZn in an aqueous solution of FS-1620 (see Supporting Material, Scheme S1) followed by bentonite adsorption. Thus, a solution 2 mg of F_{64}PcZn in 1 mL of methanol was added in 0.1 mL portions to a solution of 20 μl of FS-1620 in 10 mL of water while stirring vigorously. 100 mg of bentonite was added next and the suspension was stirred in the absence of light for 30 min, centrifuged, and the solid washed with water until no F_{64}PcZn was detected in solution via UV–vis at λ = 685 nm. F_{64}PcZn∈Ben was then dried in a vacuum oven at 40 °C overnight. The content of F_{64}PcZn in F_{64}PcZn∈Ben is about 2% (w/w).

2.3. Instrumental analyses

UV–vis and FTIR spectra were acquired at room temperature using HP8452A and Bruker IFS 48 spectrophotometers, respectively. The steady-state fluorescence spectra were recorded using a Perkin-Elmer LS-55 spectrofluorimeter.

XRD patterns were obtained with a Philips X'Pert diffractometer using CuKα radiation (40 kV and 30 mA, λ = 1.5418 Å). The diffractometer was equipped with a PW3020 vertical goniometer, a 1° divergence slit, 0.2 mm receiving slit, incident and diffracted beam Sollers, 1° anti scatter slit. The data was obtained by scanning from 2° to 52° 2Θ at a counting speed of 0.02° step/2 s. The XRD mounts were prepared by dispersing 20–100 mg solid samples in deionized water using an ultrasonic tip, depositing the suspensions on a zero background silicon wafer followed by air-drying. The data was recorded at ambient conditions, 34–38% relative humidity. Raw bentonite was also analyzed at 64% relative humidity.

2.4. Photochemical experiments

A 500 W xenon lamp with cut-off filters λ > 630 nm and λ > 550 nm was used to irradiate F_{64}PcZn and for the determination of the quantum yield of singlet oxygen formation, respectively. Solvents were bubbled with oxygen or argon for 15 min for aerobic and anaerobic experiments, respectively. Volumes of 10 mL dispersion of F_{64}PcZn∈Ben in AO7 aqueous solution ($C_{F_{64}PcZn} = C^0_{AO7}$) or F_{64}PcZn + AO7 homogenous solutions in acetonitrile or DMF were irradiated while stirring for a predetermined period of time. The photon flow was determined using the Reineckate actinometer [29] under an argon atmosphere, the concentration of $K[Cr(NH_3)_2(SCN)_4]$ being 1.24×10^{-2} M. The reaction rate, V_r, was calculated using the equation:

$$V_r = I_{>550}\Phi_{>550}\int_{\lambda} F_{>550}(\lambda)(1-10^{-A_R(\lambda)})d\lambda \quad (1)$$

where $I_{>550}$ is the maximum intensity of light emitted by the lamp at $\lambda_{>550}$ nm, $\Phi_{>550}$ is the quantum yield of the actinometric reaction, $A_R(\lambda)$ is the absorbance of $K[Cr(NH_3)_2(SCN)_4]$, and $F_{>550}(\lambda)$ is the spectral distribution of the lamp at λ > 550 nm [30].

The quantum yield of singlet oxygen formation (Φ_Δ) was determined by measuring the 440 nm bleaching of N,N-dimethyl-4-nitrosoaniline (RNO) due to a transannular peroxide induced by the reaction of singlet oxygen with imidazole, as reported previously [31,32]. The solutions contained 40 mg of F_{64}PcZn∈Ben, 0.01 mol/dm^3 imidazole while the RNO initial concentration was 5×10^{-5} mol/dm^3. Imidazole was in large excess and the changes of RNO concentration did not exceed 10% of its initial concentration (Supporting Material, Fig. S6). RNO bleaching under these conditions is a zero order kinetics process with a slope proportional to Φ_Δ. The value of Φ_Δ was calculated as follows:

$$[\mathrm{RNO}] = [\mathrm{RNO}]_0 - I_{\mathrm{abs}}^{\mathrm{BFT}}\Phi_\Delta t \quad (2)$$

where $I_{\mathrm{abs}}^{\mathrm{BFT}} = I_{>550}\int_{\lambda} F_{>550}(\lambda)(1-10^{-A_{\mathrm{BFT}}(\lambda)})d\lambda$ and A_{BFT} (λ) is the absorbance of F_{64}PcZn∈Ben at the given wavelength (λ).

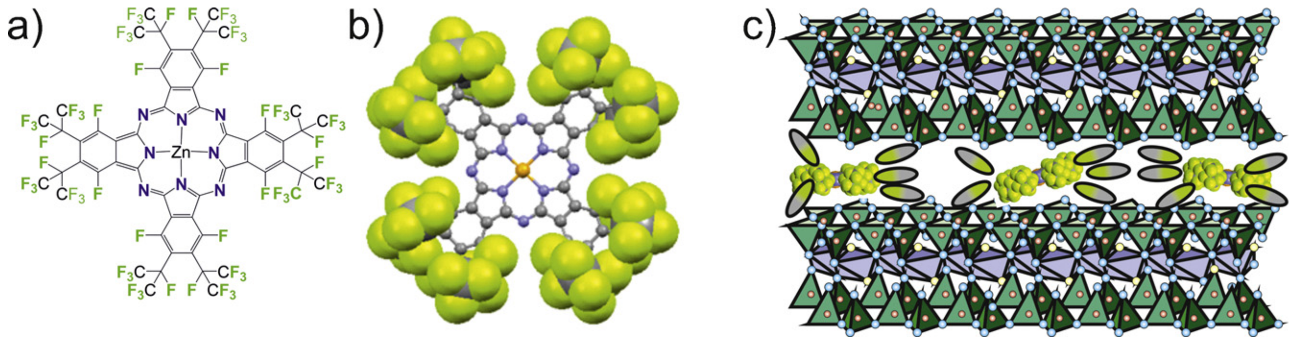

Fig. 1. (a) Structural formula of F_{64}PcZn. (b) X-ray structure of F_{64}PcZn showing the green F atoms as van der Waals spheres, while N, C, and central Zn atom are represented using a conventional ball-and-stick model. (c) Representation of $F_{64}PcZn{\in}Ben$, showing also intercalated fluoro-surfactant molecules represented as ellipsoids. See the text for details.

3. Results and discussion

The choice of organic-based photocatalysts for the degradation of pollutants poses a challenge since such materials are inherently unstable, either alone or in combination with inorganic matrices.

F_{64}PcZn (Fig. 1a), used in this study was chosen as the photosensitizer because of its very attractive spectral and photophysical/photochemical properties: it absorbs light in the visible spectral region, is an efficient generator of singlet oxygen, and, being the electron deficient molecule, it readily participates in photoinduced electron transfer processes. Additionally, this bulky molecule is not prone to aggregation [26]. What is important in view of photochemical applications is its exceptional photostability, both in the oxygen-free atmosphere and in the presence of oxygen.

F_{64}PcZn is only sparingly soluble in water, which makes it impractical as a photosensitizer in homogenous reactions in aqueous media, but this property advantageously prevents its leaching in solution in case the material is heterogenized. Consequently, we have incorporated F_{64}PcZn into smectite interlayers in bentonite, a clay that serves as a support for the photoactive dye (Fig. 1c). While phthalocyanines incorporation into the galleries of cationic and anionic clays via ion exchange and in situ crystallization of synthetic clay layers has been reported [33] there is little information on the properties of these materials. Moreover, the successful incorporation of a perfluorinated phthalocyanine in clays appears unprecedented. The current development of a method for intercalation of bentonite with F_{64}PcZn resulted in an easy and efficient procedure for materials synthesis while taking advantage of the known properties of bentonite as an adsorbent for AO7 for increasing the efficiency of its photosensitized degradation.

4. Structure and spectroscopic properties of $F_{64}PcZn{\in}Ben$ photosensitizer

XRD was used to obtain structural information regarding $F_{64}PcZn{\in}Ben$. Ben is rich in swelling 2:1 phyllosilicate (smectite), but contains also admixtures of kaolinite, quartz, and calcite (Supporting Material, Fig. S1). The presence of calcite in the raw material indicates that the smectite is most likely in the Ca-form. The $d_{(001)}$ distance of smectite was found to depend on the relative humidity (RH) [34–36]. At 38% RH the structure is dominated by 1 W layer within the interlayer spaces, while at 64% RH – 2 W layer complexes prevail (Supporting Material, Fig. S2). The mineral does not give a rational series of reflections at neither 38% nor 64% RH, a fact which is due to the coexistence of 0 W, 1 W, and 2 W interlayer complexes.

Treatment of Ben with FS-1620 affected the interplanar $d_{(001)}$ distance of the swelling 2:1 phyllosilicate (smectite) as evidenced by comparing the XRD patterns recorded at the same RH of raw vs. surfactant treated Ben samples, Fig. 2. The increase in $d_{(001)}$ distance from 12.7 Å for Ben to 14.0 Å for surfactant treated Ben indicates that the FS-1620 molecules have intercalated, most likely via exchanging the smectite interlayer cations. It is noteworthy, however, that the surfactant-saturated smectite did not produce rational series of reflections. Subsequent treatment of the Ben-FS-1620 sample with F_{64}PcZn resulted in further increase of the $d_{(001)}$ distance 14.8 Å suggesting that F_{64}PcZn also penetrated the interlayer space of the smectite. The subsequent saturation with the dye did not produce rational series of reflections. Such a small increase of $d_{(001)}$ after intercalation of the dye may be due to the fact that it is a planar molecule. Similar results have been also found for aluminum phthalocyanine intercalated into bentonite [24].

In order to gain insights into the potential photocatalytic properties of intercalated F_{64}PcZn, its light absorbing properties in solution and in confined environments were compared. In addition, we have considered the effects of the fluorosurfactant, assumed to interact directly with the fluorinated complex via its fluorinated moieties, as shown schematically in Fig. 1c.

The absorption spectra of F_{64}PcZn dissolved in organic solvents such as acetone, chloroform, and spectrograde DMF [37] and acetonitrile differ significantly from those of the same complex solubilized in the aqueous solution of FS-1620 (Fig. 3). The spectra in organic solvents are similar, exhibiting molar extinction coefficients (ε) of about 10^4–10^5.

The absorption bands of F_{64}PcZn, especially those at longer wavelengths ($\pi \rightarrow \pi^*$ Q band), are broader for F_{64}PcZn solubilized in FS-1620 compared to F_{64}PcZn dissolved in acetonitrile, acetone, DMF, and chloroform. Interestingly, no spectral broadening is observed in fluorinated solvents (Supporting Material, Fig. S3) and the addition of water to fluorinated solvents to yield a biphasic mixture does not broaden the F_{64}PcZn spectra, either. No additional spectral features that can be attributed to the significant formation of dimers could be identified.

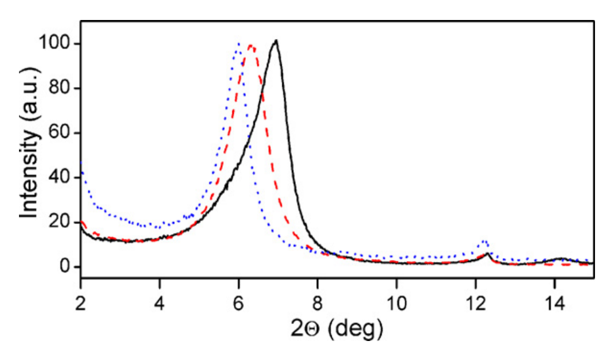

Fig. 2. XRD patterns of raw (solid line), FS-1620-treated (dashed line), and F_{64}PcZn–FS–1620-intercalated (dotted line) bentonite sample.

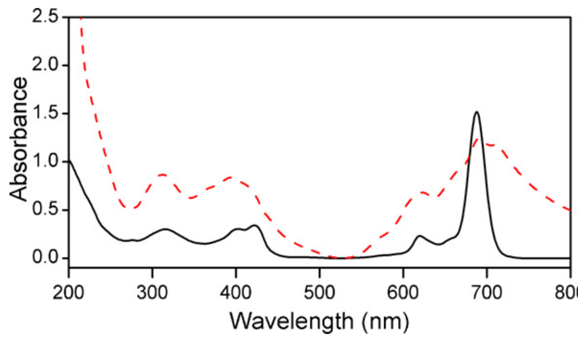

Fig. 3. UV–vis spectra of $F_{64}PcZn$ in MeCN ($c_{F_{64}PcZn} = 2.3 \times 10^{-5}$ mol/dm^3, solid) and solubilized in the aqueous solution of FS-1620 (dashed) ($c_{F_{64}PcZn} = 1.3 \times 10^{-4}$ mol/dm^3, $c_{FS-1620}$ = 20 µl/10 ml).

The fluorescence emission spectra of $F_{64}PcZn$ solubilized in FS-1620 ($c_{FS-1620}$ = 20 µl/10 ml) are also shifted to longer wavelengths compared to those for $F_{64}PcZn$ dissolved in acetonitrile (Fig. 4), a phenomenon also observed in CCl_4 and liposomes [38]. Differences in the absorption and emission spectra of $F_{64}PcZn$ in acetonitrile and solubilized by FS-1620 may be due to the different chromophore–solvent interactions, which is of hydrocarbon and fluorocarbon type, respectively, although it should be noted the spectra of $F_{64}PcZn$ in fluorinated solvents appear no different than those in hydrocarbons or even liposomes.

The efficiency of incorporation of $F_{64}PcZn$ solubilized by FS-1620 into Ben was probed by UV–vis since neither Ben nor FS-1620 absorb light above 300 nm (Supporting Material, Fig. S4). Thus, the UV–vis spectrum of the solution, left after the removal of suspended Ben equilibrated with $F_{64}PcZn$ solubilized by FS-1620, showed no residual $F_{64}PcZn$, which is consistent with the formation of $F_{64}PcZn{\in}Ben$ indicated by XRD measurements.

5. $F_{64}PcZn{\in}Ben$ photosensitized degradation of AO7

The spectroscopic monitoring of the degradation of AO7 by an aqueous suspension of $F_{64}PcZn{\in}Ben$ is shown in Fig. 5.

The AO7 degradation was followed by the measurement of the decrease of its absorption at λ = 486 nm. The addition of $F_{64}PcZn{\in}Ben$ to AO7 solution resulted in a decrease in its concentration in solution even before irradiation was started. This indicated that AO7 was strongly adsorbed by $F_{64}PcZn{\in}Ben$ (Fig. 5a). Consequently, the irradiation experiments were conducted after 30 min pre-equilibration, a time sufficient for the UV–vis spectrum to remain unchanged. Irradiation of the equilibrated AO7 solution for 2 h resulted in almost complete disappearance of the 486 nm absorption band characteristic of AO7 (Fig. 5b). Further

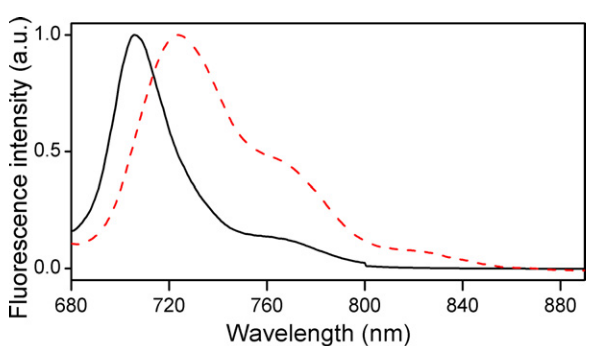

Fig. 4. Normalized fluorescence emission spectra of $F_{64}PcZn$ dissolved in MeCN (solid) and solubilized in the aqueous solution of FS-1620 (dashed) ($C_{F_{64}PcZn} = 1.3 \times 10^{-5}$ mol/dm^3, $C_{FS-1620}$ = 20 µl/10 ml, λ_{ex} = 660 nm).

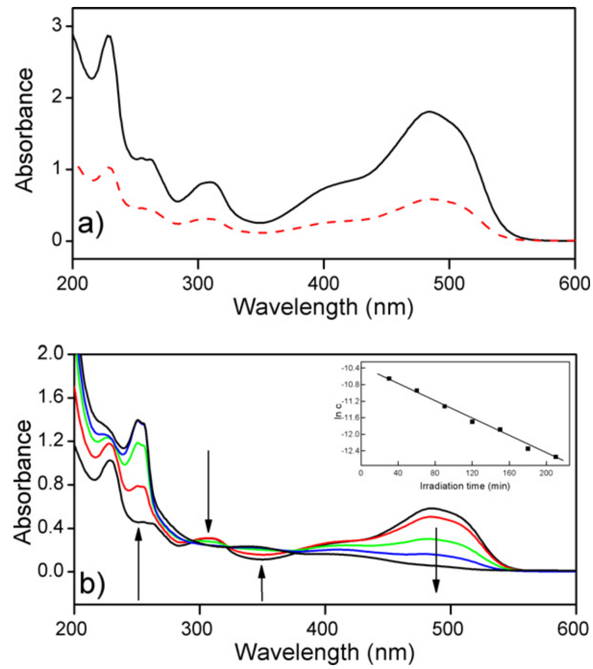

Fig. 5. (a) UV–vis spectra of an AO7 solution prior to (solid-line) and 30 min after addition of $F_{64}PcZn{\in}Ben$. The photocatalyst was removed by centrifugation; (b) UV–vis of oxygenated solution of AO7 irradiated with λ_{irr} > 630 nm in the presence of $F_{64}PcZn{\in}Ben$ recorded after 0, 30, 60, 90, and 120 min. Insert: the λ = 486 nm intensity fitted to a first order kinetic equation (see Supporting Material) ($c_{AO7} = 1.0 \times 10^{-4}$ mol/dm^3, $c_{Ben\text{-}F_{64}PcZn}$ = 1 g/dm^3, λ_{irr} > 630 nm).

irradiation did not cause any noticeable changes in the spectra. Since the adsorbed and dissolved forms of AO7 are in the equilibrium and no AO7 was present in the solution after irradiation, it could be concluded that practically all AO7 present in the system was degraded.

To elucidate the effect of oxygen on the degradation process the AO7 + $F_{64}PcZn{\in}Ben$ system was saturated with argon and irradiated under the same conditions. It was observed that AO7 undergoes degradation also in an oxygen-free atmosphere, although the process is slower (Fig. 6). Interestingly, the processes occurring in the presence and in the absence of oxygen can be described by a first order kinetic equation (see insert in Fig. 6).

Since there was no degradation of AO7 in the absence of photosensitizer and $F_{64}PcZn$ did not undergo photoreaction upon irradiation, both the aerobic an anaerobic degradation processes are photosensitized.

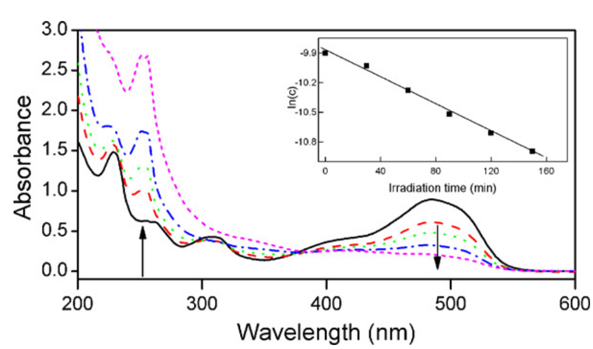

Fig. 6. UV–vis spectra of solution of AO7 containing $F_{64}PcZn{\in}Ben$ irradiated for 0, 60, 90, 150, and 300 min in the absence of oxygen. Insert: first order kinetic equation fit (see Supporting Material) ($C_{AO7} = 2.0 \times 10^{-4}$ mol/dm^3, $C_{Ben\text{-}F_{64}PcZn}$ = 1 g/dm^3, λ_{irr} > 630 nm).

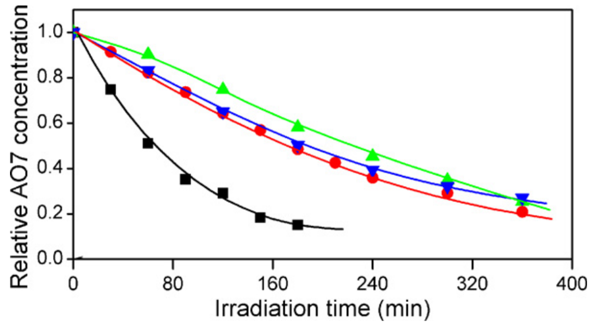

Fig. 7. Dependence of the relative AO7 concentration on irradiation time for AO7 solutions irradiated in the presence of the same sample of Ben-F_{64}PcZn used 1 (■), 2 (●), 3 (▲), and 4 times (▼).

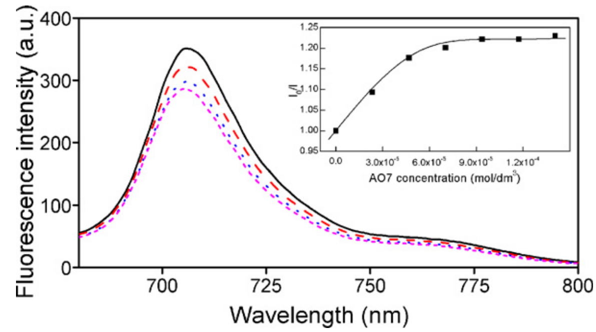

Fig. 8. Fluorescence emission spectra of F_{64}PcZn solutions in MeCN containing 0 (solid), 2.34×10^{-5} (dashed), 4.69×10^{-5} (dotted), and 14.06×10^{-5} (small dash) mol/dm^3 of AO7 (λ_{ex} = 660 nm). Insert: corresponding Stern–Volmer plot.

Furthermore, the heterogenized system appears suitable for practical applications. Thus, F_{64}PcZn∈Ben was suspended in AO7 solution, irradiated, removed by centrifugation, added to fresh AO7 solution, and irradiated again. This procedure was repeated four times and the changes of AO7 concentration on irradiation time in each cycle were monitored (Fig. 7). There is a decrease in the photodegradation rate between the first and the second cycle, but during the second, third, and fourth cycle the reaction rates are similar. The results suggest that the dye underwent a transformation during the 1st cycle, for example internal equilibrium, removal of adventitious adsorbed species, etc., reaching compositional parameters that remain invariable during next cycles. The exact nature of the transformation is, however, unknown.

In summary, F_{64}PcZn∈Ben is a stable, recyclable photocatalyst.

6. Mechanism of F_{64}PcZn∈Ben photosensitized degradation of AO7

The first hypothesis, based on the role of similar materials in clays as well as the previously reported reactivity of F_{64}PcZn [39], is that singlet oxygen is involved in the AO7 photosensitized degradation. Previous studies indicated that AO7 reacts with singlet oxygen [18,40]. The proposed mechanism of AO7 oxidation (Supporting Material, Scheme S2) is based on the general mechanism for oxidation of 1-aryl azo-2-naphthols proposed by Griffiths and Hawkins [41].

The addition of NaN_3, a well-known $^1O_2$ quencher, to our system resulted in the complete inhibition of AO7 photodecomposition. Moreover, the water soluble specific singlet-oxygen acceptor, 2-anthracene sulfonate (ANS) was photooxidized, a process that does not proceed in the absence of F_{64}PcZn∈Ben (see Supporting Material, Fig. S5). The quantum yield of singlet oxygen production, Φ_Δ, determined as described in the Experimental section, was 0.170 ± 0.001, a value similar to the 0.126 value determined for liposome-encapsulated F_{64}PcZn.

It is interesting to note that the value of Φ_Δ is strongly dependent on the environment and equals to 0.606 in methanol [38], 0.21 in acetone [39], and 0.81 in ethanol [26]. Taken together, the above data prove singlet oxygen participation in the decomposition of AO7 by F_{64}PcZn∈Ben and thus the ability of F_{64}PcZn to retain its photosensitizing activity not only in liposomes but also in clays.

The singlet-oxygen based decomposition pathway, however, is not unique. Thus, F_{64}PcZn∈Ben is able to decompose AO7 in argon via an anaerobic, redox pathway. The primary photophysical step of F_{64}PcZn-photosensitized degradation of AO7 is proposed to be a photoinduced electron transfer from AO7 to electron deficient molecule of F_{64}PcZn.

The proposal is based on the fact that F_{64}PcZn, an electron deficient compound, was shown to easily undergo reduction in one-electron transfer processes [37]. The F_{64}PcZn photosensitized degradation process of AO7 was carried out in two solvents of similar polarity but different viscosity, namely acetonitrile (ε = 35.94, $\eta = 0.345 \times 10^{-3}$ Pa s at 25 °C [42]) and DMF (ε = 36.71, $\eta = 0.924 \times 10^{-3}$ Pa s at 25 °C [42]). Irradiation of F_{64}PcZn and AO7 in deoxygenated acetonitrile solution resulted in AO7 bleaching (Supporting Material, Fig. S7). The kinetics of that process obeys the second order equation. Additionally, the measurement of F_{64}PcZn fluorescence in the absence and in the presence of AO7 indicated that AO7 quenches the excited singlet state of F_{64}PcZn in acetonitrile solution (Fig. 8).

The quenching cannot occur via energy transfer (energies of F_{64}PcZn and AO7 singlet states are $E_{F_{64}PcZn} = 1.80$ eV [37] and $E_{AO7} = 2.36$ eV [43], respectively), therefore one can assume that it occurs via photoinduced electron transfer. To determine whether such process is thermodynamically possible, ΔG was calculated using the Rehm–Weller equation:

$$\Delta G^0 = E_D^o - E_A^{red} - E^* - C \quad (3)$$

where E_D^o is the oxidation potential of the electron donor, (E_D^o = 0.76 eV) for AO7 [44], E_A^{red} is the reduction potential of the electron acceptor ($E_A^{red} = -0.25$ eV) [45], E^* is the energy of the electronically excited-state of donor (E^* = 1.80 eV for F_{64}PcZn) [37] and C is an electrostatic correction term, which is typically equal to 0.1 eV for a polar solvent. Using these values one can find that $\Delta G = -0.89$ eV, i.e., the process is thermodynamically favorable and can be described as follows:

$$^1F_{64}PcZn* + AO7 \rightarrow F_{64}PcZn^{\bullet -} + AO7^{\bullet +} \quad (4)$$

However, fitting of the quenching data to the typical Stern–Volmer plot indicated that the expected linear dependence is observed only for the concentration of AO7 lower than 8×10^{-5} mol/dm^3. The quenching becomes less efficient at higher concentration of AO7 (Fig. 8, insert). This suggests that the electron transfer occurs via encounter complex between electron donor and acceptor, a reversible process that allows the occurrence of secondary reactions only when the initially formed radical ions can be separated (spatially or by solvent cage formed by the molecules of polar solvents). A similar quenching process has been reported for the quenching of excited states of quinones by polymethylbenzenes [46].

Interestingly, the studies carried out in DMF have shown that although the fluorescence of F_{64}PcZn is quenched by AO7, no products are formed on irradiation of F_{64}PcZn + AO7 in argon. Since polarities of MeCN and DMF are similar, that difference might be explained considering the differences in solvent viscosities. Namely, in much less viscous MeCN the radical ions formed can quickly separate from each other by diffusion before the back electron transfer can take place, and then undergo irreversible secondary reactions, resulting in AO7 degradation. On the other hand,

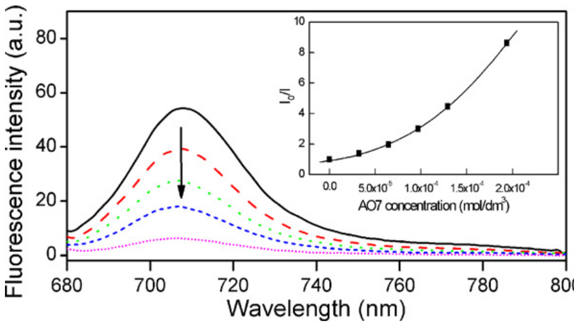

Fig. 9. F_{64}PcZn fluorescence quenching by AO7 in DMF (argon atmosphere). Insert: corresponding Stern–Volmer plot.

in more viscous DMF the back electron transfer occurs before the radical ions diffuse out thus no net reaction can be observed.

The rate constant for the electron transfer in F_{64}PcZn + AO7 in MeCN determined from the linear part of the Stern–Volmer plot is $k_q = 5 \times 10^6\ M^{-1}\ s^{-1}$. The value is quite low reflecting the postulated above formation of encounter complex and/or solvent cage effect. Additionally, in DMF, a more viscous solvent, the fluorescence of F_{64}PcZn is quenched according to mixed dynamic/static mechanisms (Fig. 9). Most likely, the charge recombination within the solvent cage occurs and there is no secondary product formation.

In the presence of oxygen, the F_{64}PcZn photosensitized oxidation of AO7 occurs in both solvents, although the rate of the reaction in DMF is considerably lower than that in MeCN. The difference in efficiency of the reactions most likely reflects the difference in Φ_Δ and the lifetime of $^1O_2$ in these solvents; $\tau = 30\ \mu s$ in MeCN and $\tau = 19\ \mu s$ in DMF.

7. Conclusions

In conclusion, we have reported a new, efficient photosensitizer F_{64}PcZn∈Ben. The material is active under visible light illumination and can be used to photosensitize degradation of AO7 in water by producing $^1O_2$ as well as via a photoinduced electron transfer.

Acknowledgements

The authors gratefully acknowledge the financial support of Polish Ministry of Science and Higher Education in form of the grant No. N N209144436 as well as that of the United States Department of Defense. DD is grateful to Dr. Mariusz Kępczyński for his help in photochemical calculations.

Appendix A. Supplementary data

Supplementary data associated with this article can be found, in the online version, at http://dx.doi.org/10.1016/j.apcatb.2012.05.021.

References

[1] H. Zollinger, Color Chemistry: Synthesis, Properties and Applications of Organic Dyes and Pigments, VCH Publishers, New York, 1991.
[2] M. Jonstrup, M. Punzi, B. Mattiasson, Journal of Photochemistry and Photobiology A 224 (2011) 55–61.
[3] S. Nadupalli, N. Koorbanally, S.B. Jonnalagadda, Journal of Physical Chemistry A 115 (2011) 11682–11688.
[4] C.A. Castro, A. Centeno, S.A. Giraldo, Materials Chemistry and Physics 129 (2011) 1176–1183.
[5] Z. Ai, J. Li, L. Zhang, S. Lee, Ultrasonics Sonochemistry 17 (2010) 370–375.
[6] D. Prato-Garcia, G. Buitrón, Water Science and Technology 59 (2009) 965–972.
[7] M.A. Rauf, M.A. Meetani, S. Hisaindee, Desalination 276 (2011) 13–27.
[8] O. Legrini, E. Oliveros, A.M. Braun, Chemical Reviews 93 (1993) 671–698.
[9] M.R. Hoffmann, S.T. Martin, W. Choi, D.W. Bahnemann, Chemical Reviews 95 (1995) 69–96.
[10] K. Vinodgopal, P.V. Kamat, Journal of Physical Chemistry 96 (1992) 5053–5059.
[11] C. Nasr, K. Vinodgopal, L. Fisher, S. Hotchandani, A.K. Chattopadhyay, P.V. Kamat, Journal of Physical Chemistry 100 (1996) 8436–8442.
[12] F. Zhang, J. Zhao, L. Zang, T. Shen, H. Hidaka, E. Pelizzetti, N. Serpone, Journal of Molecular Catalysis A: Chemical 120 (1997) 173–178.
[13] F. Zhang, J. Zhao, T. Shen, H. Hidaka, E. Pelizzetti, N. Serpone, Applied Catalysis B: Environmental 15 (1998) 147–156.
[14] G. Liu, T. Wu, J. Zhao, H. Hidaka, N. Serpone, Environmental Science and Technology 33 (1999) 2081–2087.
[15] T. Wu, G. Liu, J. Zhao, H. Hidaka, N. Serpone, Journal of Physical Chemistry B 103 (1999) 4862–4867.
[16] T. Wu, T. Lin, J. Zhao, H. Hidaka, N. Serpone, Environmental Science and Technology 33 (1999) 1379–1387.
[17] J. Bandara, J.A. Mielczarski, J. Kiwi, Langmuir 15 (1999) 7670–7679.
[18] M. Stylidi, D.I. Kondarides, X.E. Verykios, Applied Catalysis B: Environmental 47 (2004) 189–201.
[19] P. Ji, J. Zhang, F. Chen, M. Anpo, Applied Catalysis B: Environmental 85 (2009) 148–154.
[20] N. Daneshvar, S. Aber, F. Hosseinzadeh, GLOBAL NEST Journal 10 (2008) 16–23.
[21] S.A. Hassan, F.Z. Yehia, A.A. Hamed, A.A. Zahran, S.M. Solyman, Journal of Porous Materials 18 (2011) 1–11.
[22] S.A. Sadek, S.M. Solyman, H.S. Abdel-Samad, S.A. Hassan, International Journal of Polymeric Materials 59 (2010) 353–369.
[23] S.A. Hassan, A.A. Zahran, F.Z. Yehia, Adsorption Science and Technology 20 (2002) 269–284.
[24] Z. Xiong, Y. Xu, L. Zhu, J. Zhao, Environmental Science and Technology 39 (2005) 651–657.
[25] Z. Xiong, Y. Xu, L. Zhu, J. Zhao, Langmuir 21 (2005) 10602–10607.
[26] R. Gerdes, Ł. Łapok, O. Tsaryova, D. Wöhrle, S.M. Gorun, Dalton Transactions 7 (2009) 1098–1100.
[27] C. Keil, O. Tsaryova, Ł. Łapok, C. Himcinschi, D. Wöhrle, O.R. Hild, D.R.T. Zahn, S.M. Gorun, D. Schlettwein, Thin Solid Films 517 (2009) 4379–4384.
[28] E.E. Wegner, A.W. Adamson, Journal of the American Chemical Society 88 (1966) 394–404.
[29] J.F. Rabek, Experimental Methods in Photochemistry and Photophysics, Wiley and Sons, Chicester, 1982.
[30] M. Kępczyński, A. Czosnyka, M. Nowakowska, Journal of Photochemistry and Photobiology A 185 (2007) 198–205.
[31] E. Gandin, Y. Lion, A. Van de Vorst, Photochemistry and Photobiology 37 (1983) 271–278.
[32] I. Kraljić, E. Mohsni, Photochemistry and Photobiology 28 (1978) 577–581.
[33] K.A. Carrado, J.E. Forman, R.E. Botto, R.E. Winans, Chemistry of Materials 5 (1993) 472–478.
[34] E. Ferrage, B. Lanson, B.A. Sakharov, V.A. Drits, American Mineralogist 90 (2005) 1358–1374.
[35] E. Ferrage, B. Lanson, B.A. Sakharov, N. Geoffroy, E. Jacquot, V.A. Drits, American Mineralogist 92 (2007) 1731–1743.
[36] E. Ferrage, B. Lanson, L.J. Michot, J.-L. Robert, Journal of Physical Chemistry C 114 (2010) 4515–4526.
[37] S.P. Keizer, J. Mack, B.A. Bench, S.M. Gorun, M.J. Stillman, Journal of the American Chemical Society 125 (2003) 7067–7085.
[38] R. Minnes, H. Weitman, H.-J. Lee, S.M. Gorun, B. Ehrenberg, Photochemistry and Photobiology 82 (2006) 593–599.
[39] A.C. Beveridge, B.A. Bench, S.M. Gorun, G.J. Diebold, Journal of Physical Chemistry A 107 (2003) 5138–5143.
[40] F. Ruyffelaere, V. Nardello, R. Schmidt, J.-M. Aubry, Journal of Photochemistry and Photobiology A 183 (2006) 98–105.
[41] J. Griffiths, C. Hawkins, Journal of the Chemical Society, Perkin Transactions 2 6 (1977) 747–752.
[42] L. Murov, Handbook of Photochemistry, 2nd ed., Marcel Dekker Inc., New York, 1993.
[43] K. Vinodgopal, P.V. Kamat, Journal of Photochemistry and Photobiology A: Chemistry 83 (1994) 141–146.
[44] K. Vinodgopal, P.V. Kamat, Environmental Science and Technology 29 (1995) 841–845.
[45] B.A. Bench, W.W. Brennessel, H.-J. Lee, S.M. Gorun, Angewandte Chemie International Edition 41 (2002) 750–754.
[46] S.M. Hubig, J.K. Kochi, Journal of the American Chemical Society 121 (1999) 1688–1694.